Synergy between FATP2 and RIPK3 pathways promotes PMN-MDSCs-potentiated suppressive immunity in bladder cancer

Xiaojun Shi (1105405029@qq.com)
Southern Medical University Nanfang Hospital https://orcid.org/0000-0003-1125-6725
Shiyu Pang
Southern Medical University Nanfang Hospital
Jiawei Zhou
Southern Medical University Nanfang Hospital
Guang Yan
Southern Medical University Nanfang Hospital
Jie Sun
Southern Medical University Nanfang Hospital
Wanlong Tan
Southern Medical University Nanfang Hospital

Research Article

Keywords: PMN-MDSCs, Fatty acid transporter protein 2, Receptor-interacting protein kinase 3, Immunotherapy, Bladder cancer.

Posted Date: April 12th, 2022

DOI: https://doi.org/10.21203/rs.3.rs-1526442/v1

Abstract

Background Polymorphonuclear myeloid-derived suppressor cells (PMN-MDSCs) promote tumor immune tolerance and cause tumor immunotherapy failure. In this study, we found that high PMN-MDSCs infiltration, overexpressed fatty acid transporter protein 2 (FATP2) and underexpressed receptor-interacting protein kinase 3 (RIPK3) existed in the mouse and human bladder cancer tissues. However, the related mechanisms remain largely unknown.

Methods and results Both FATP2 and RIPK3 expressions were associated with clinical stage. FATP2 knockout or up-regulating RIPK3 reduced the synthesis of prostaglandin E2 (PGE2) in PMN-MDSCs, attenuated the suppressive activity of PMN-MDSCs on $CD8^+$ T cells functions and inhibited the tumor growth. There was a PGE2-mediated synergy between FATP2 and RIPK3 pathways, which markedly promoted the immunosuppressive activity of PMN-MDSCs. Combination therapy with inhibition of FATP2 and activation of RIPK3 can effectively inhibit tumor growth.

Conclusions This study demonstrated that a synergy between FATP2 and RIPK3 pathways in PMN-MDSCs significantly promoted the synthesis of PGE2, which severely impaired the $CD8^+$ T cell functions. This study may provide new ideas for immunotherapy of human bladder cancer.

Introduction

Bladder cancer (BCa) is one of the most common malignancies and has a high recurrence rate [1]. One of the important reasons for the difficulty in controlling tumors is that tumor cells continue to grow by evading the killing effect of immune cells through immune escape mechanisms [2]. Polymorphonuclear myeloid-derived suppressor cells (PMN-MDSCs) is pathologically activated neutrophils that accumulate in many diseases [3]. PMN-MDSCs infiltration is one of the most important causes for tumor progression and therapeutic failure, and their presence correlates with poor prognosis [4]. PMN-MDSCs can induce immune tolerance by overexpressing arginase 1 (Arg-1), inducible nitric oxide synthase (iNOS), and reactive oxygen species (ROS) [5]. The mechanisms responsible for pathological activation of neutrophils remain largely unknown. With the discovery of the molecular marker (LOX-1 protein) [6], PMN-MDSCs can be distinguished from other neutrophils, thereby promoting the related research on the regulatory mechanism of PMN-MDSCs functions.

Both Fatty acid transporter protein 2 (FATP2) and receptor-interacting protein kinase 3 (RIPK3) are important regulatory molecules for MDSCs to exert immunosuppressive functions [7,8]. FATP2 is a long-chain fatty acid transporter and acetyl-CoA synthetase and promotes oxidation of fatty acids and lipid synthesis [9]. As confirmed by a previous study, FATP2 enhanced the immune suppressive activity of PMN-MDSCs by promoting the synthesis of prostaglandin E2 (PGE2) [7]. In addition, RIPK3 also has important regulatory roles in tumor immunity.[10,11] Yan et al. firstly reported a RIPK3-PGE2 circuit in PMN-MDSCs, which significantly promoted the synthesis of PGE2, thereby greatly enhancing the immunosuppressive activity of PMN-MDSCs [8].

In this study, we found that the bladder tumor tissue was infiltrated with a large number of PMN-MDSCs. Moreover, the FATP2 expression was up-regulated, and the RIPK3 expression was down-regulated. The PMN-MDSCs infiltration was positively correlated with the FATP2 expression and negatively correlated with RIPK3 expression. However, it is unclear whether there is an interaction between the FATP2 and the RIPK3 pathways. Therefore, the aim of this study was to elucidate a synergy between the FATP2 and the RIPK3 pathways in promoting the immunosuppressive activity of PMN-MDSCs. Addressing the mechanisms regulating MDSCs will provide new ideas for the immunotherapy of bladder cancer.

Materials And Methods

Human samples

Samples of tumor tissues were collected from 18 patients with stage I-IV bladder cancer at Nanfang hospital of Southern Medical University (Guangzhou, China). This cohort includes 12 females and 6 males. The age ranged from 42 to 70 years. The study was approved by the Ethics Committee of Nanfang hospital. All patients signed the approved consent forms.

Animals and cells

The mouse bladder cancer cell line was obtained from the ATCC. MycoplasmaOUT (Genloci) was used to protect the cells against mycoplasma contamination. All cell lines used in this study have been authenticated every six months. C57BL/6 mice were obtained from the experimental animal center of Southern Medical University (Guangzhou, China). FATP2 knockout (KO) C57BL/6 mice generated using CRISPR-Cas9 genome-editing system were kindly provided by Guanxin Wang (Sun Yat-sen University, Guangzhou, China).

Animal experiments

Animal experiments were approved by Animal Care and Use Committee of Southern Medical University (Ethical number: L2018113). All wild-type (WT) and KO C57BL mice were randomly assigned to the treatment groups. Subcutaneous models of bladder cancer were established by injecting subcutaneously with mouse bladder cancer cell lines. For some indicated experiments, lipofermata or 666 − 15 was injected intraperitoneally every 2 days until the mice were sacrificed. Tumor size was measured with calipers. Tumors and spleens were removed upon sacrifice at indicated interval. All experimental procedures were performed in accordance with the relevant laws and institutional guidelines of Southern Medical University.

Immunofluorescence

Tumor tissues were embedded in freeze embedding medium. The frozen sections were fixed and incubated with anti-CD11b (eBioscience) and anti-LOX-1 antibodies (eBioscience) for 60 minutes. The secondary antibodies (Alexa Fluor 647-labeled goat anti-rabbit Abs and Alexa Fluor 488-labeled goat anti-rat Abs)(eBioscience) were then added and incubated for 30 minutes. The slides were mounted with a

Vectashield DAPI-containing kit. Then $CD11b^+LOX\text{-}1^+$ cells in the tumor tissue were visualized with fluorescence microscopy.

Immunohistochemistry

Tumor tissues were fixed, paraffin-embedded, dewaxed, rehydrated, and antigen retrieval. Then samples were incubated with anti-FATP2 or anti-RIPK3 antibody (Epitomics) for 30 minutes. The slides were washed with TBST for 5 minutes three times and incubated in secondary biotinylated antibody for 30 minutes. The positively expressed protein was visualized using the anti-rat Ig SABC kit (spring) and counter stained with hematoxylin and eosin.

Western blot analysis

Cells were lysed by RIPA lysis buffer. After protein extraction and electrophoresis, transfer to membrane and blocking, the samples were incubated with primary antibody at 4°C overnight, following by incubation with horseradish peroxidase-conjugated secondary antibodies for 1 hour at room temperature. Finally, the membranes were visualized after incubation with chemiluminescence using a Tanon 5200 system. The primary antibodies used in this experiment include anti-FATP2, anti-RIPK3, anti-PKA, anti-CREB, anti-p65, anti-COX-2 and anti-GAPDH.

Isolation of PMN-MDSCs and PMNs

Single-cell suspensions were prepared from spleen and followed by red blood cell lysed. Single-cell suspensions from tumor tissues were prepared using Tumor Dissociation Kit (Miltenyi). PMN-MDSCs and PMNs were isolated using anti-PE beads and MACS column (Miltenyi). Cells were then culture in RPMI1640 containing 10% fetal bovine serum, 1% penicillin/streptomycin and 0.1% sodium pyruvate.

$CD8^+$ T-cell isolation and proliferation assay

$CD8^+$ T cells were isolated from the spleen of C57BL/6 mice by $CD8^+$ T Cell Enrichment Kit (BioLegend). PMN-MDSCs were isolated from the tumor or spleen of C57BL/6 mice by magnetic beads (BioLegend). PMN-MDSCs were then cocultured with CFDA-SE (Carboxyfluorescein diacetate, succinimidyl ester) labeled $CD8^+$ T cells in the medium containing anti-CD3 (1 μg/mL) and anti-CD28 (1 μg/mL) antibodies (BD Biosciences) for 72 hours. To enumerate the $CFSE^+CD8^+$ and IFN-γ^+CD8^+ T-cell subset, cells were first stained with FITC-labeled anti-mCD8 (Biolegend), then fixed or permeabilized before they were stained with PE-labeled anti-IFN-γ antibody (Biolegend). The $CFSE^+CD8^+$ and IFN-γ^+CD8^+ T cells were detected by flow cytometry (Becton Dickinson, San Jose, CA, USA).

Quantitative real-time PCR

Total RNA from cells was extracted using the Arcturus PicoPure RNA isolation kit (Biosciences). cDNA was synthesized with Reverse Transcription system (Toyobo). Real-time PCR was performed using SYBR Green PCR Master Mix (Applied Biosystems). Normalization and fold changes were calculated using the ΔΔCt method, and GAPDH was used as negative control.

Liquid chromatography-mass-spectrometry of lipids (LC-MS)

PMN-MDSCs and PMNs were isolated by the methods described above. Cells were then cultured in RPMI1640 for 48 hours. The supernatants were collected for evaluating lipids and PGE2 concentrations. Extracted samples were separated by an Acquity UPLC system (Waters). Lipids and PGE2 were analyzed using scheduled multiple reaction monitoring (MRM). Analysis of LC-MS data acquisitions were performed using Analyst 1.6.2 software (Applied Biosystems).

ELISA

PMN-MDSCs and PMNs were isolated by the methods described above. Cells were then cultured in RPMI1640 containing 10% fetal bovine serum, 1% penicillin/streptomycin and 0.1% sodium pyruvate. The supernatant was harvested by centrifugation. According to the manufacturer's instructions, the concentrations of Arg-1, IL-10 and iNOS were measured by ELISA (R & D Systems, Minneapolis, MN).

Statistics

Immunohistochemistry, immunofluorescence, FACS, qPCR, LC-MS and ELISA data were analyzed using T test or one-way ANOVA. The tumor volume data was analyzed using repeated measures design. All analyses were performed using SPSS (version 19.0). $P < 0.05$ was considered indicative of statistical significance.

Results

PMN-MDSCs, overexpressed FATP2 and underexpressed RIPK3 in the tumor tissues

Tumor tissues were collected to detect PMN-MDSCs infiltration, FATP2 and RIPK3 expression. The double positive cells ($CD11b^{+}LOX\text{-}1^{+}$) were considered PMN-MDSCs, which were visualized with fluorescence microscopy. FATP2 and RIPK3 expression were display by immunohistochemistry. As shown in Fig. 1A, a large number of PMN-MDSCs existed in the tumor tissues. FATP2 expression was significantly up-regulated, and RIPK3 expression was significantly down-regulated (Fig. 1B, C). The results of statistical analysis showed that the number of PMN-MDSCs in the tumor tissues was positively correlated with FATP2 expression and negatively correlated with RIPK3 expression (Fig. 1D, E). To confirm whether this phenomenon also exists in the tumor tissues of human bladder cancer, clinical bladder cancer tissue were collected. Immunohistochemical results showed that the expressions of LOX-1 and FATP2 in human bladder cancer tissue were higher than that in adjacent tissues, and the RIPK3 expression was lower than that in adjacent tissues (Fig. 1F). Moreover, the expression of FATP2 in patients with stage III/IV bladder cancer was higher than that in stage I/II, while the RIPK3 expression showed the opposite result (Fig. 1G).

Overexpressed FATP2 and underexpressed RIPK3 in PMN-MDSCs

To further evaluate the aberrantly expressed FATP2 and RIPK3 in PMN-MDSCs, we compared PMN-MDSCs isolated from tumor-bearing mice with PMNs isolated from normal mice. FATP2 and RIPK3 expression in PMN-MDSCs or PMNs were detected by immunohistochemistry, lipid metabolism-related molecules were detected by LC-MS, and immunosuppressive factors were detected by ELISA. As shown in Fig. 2A, the FATP2 expression in PMN-MDSCs of tumor-bearing mice was higher than that in PMNs of normal mice. Moreover, the PMN-MDSCs isolated from tumor tissues showed higher FATP2 expression than that isolated from spleen. The RIPK3 expression in PMN-MDSCs of tumor-bearing mice was lower than that in PMNs of normal mice, and the PMN-MDSCs isolated from tumor tissues showed lower RIPK3 expression than that isolated from spleen (Fig. 2B). The concentrations of lipid metabolism-related molecules (triglycerides (TG), arachidonic acid (AA), PGE2) and immunosuppressive molecules (Arg-1, INOS, IL-10) in the PMN-MDSCs of tumor-bearing mice were significantly higher than those in the PMNs of normal mice (Fig. 2C,D).

Effects of FATP2 KO on the functions of PMN-MDSCs.

To investigate the effect of FATP2 on lipid metabolism and immunosuppressive activity of PMN-MDSCs, FATP2 gene (SLC27A2) was knocked out with CRISPR/Cas9. As shown in Fig. 3A, Western blotting and RT-qPCR showed the results of SLC27A2 knockout. FATP2 KO reduced the concentrations of lipid metabolism-related molecules (TG, AA, PGE2) in PMN-MDSCs (Fig. 3B). In addition, FATP2 KO significantly promoted the IFN-γ and Granzyme B expressions in $CD8^+$ T cells (Fig. 3C, D). As shown in Fig. 3E, FATP2 KO attenuated the suppressive activity of PMN-MDSCs on the proliferation of $CD8^+$ T cells. Finally, FATP2 KO significantly inhibited the tumor growth in tumor-bearing mice (Fig. 3F).

Effects of RIPK3-activated on the functions of PMN-MDSCs.

To investigate the effect of RIPK3 on immunosuppressive activity of PMN-MDSCs, 666 − 15 was used to activate the RIPK3 expression. RT-qPCR and western blotting showed the up-regulation of RIPK3 expression after 666 − 15 treatment (Fig. 4A). Up-regulating RIPK3 significantly reduced the concentrations of Arg-1 and PGE2 (Fig. 4B). Similar to the effect of FATP2 KO, Up-regulating RIPK3 significantly promoted the IFN-γ and Granzyme B expressions in $CD8^+$ T cells (Fig. 4C, D). As shown in Fig. 4E, FATP2 KO attenuated the suppressive activity of PMN-MDSCs on the proliferation of $CD8^+$ T cells. Finally, FATP2 KO significantly inhibited the tumor growth in tumor-bearing mice (Fig. 4F). These results indicate that both FATP2 and RIPK3 play an important role in maintaining the suppressive activity of PMN-MDSCs. As shown in Fig. 3B and Fig. 4B, FATP2 KO minimized the synthesis of PGE2 in PMN-MDSCs in vitro. However, up-regulating RIPK3 also reduced the synthesis of PGE2 in PMN-MDSCs, but it could not reduce that to the greatest extent.

Synergy between FATP2 and RIPK3 pathways was mediated through PGE2.

One of the key triggers of the RIPK3-PGE2 circuit is PGE2, which can be synthesized by PMN-MDSCs, or by other cells, such as tumor cells.[8] To investigate whether there was a synergy between FATP2 and

RIPK3 pathways, which was mediated through PGE2, FATP2 KO PMN-MDSCs were co-cultured with PGE2 and/or 666 − 15. As shown in Fig. 5A, FATP2 KO significantly up-regulated the RIPK3 expression. This results indicated that FATP2 KO not only reduced the synthesis of PGE2 but also broken the RIPK3-PGE2 circuit. However, as shown in Fig. 5B, adding exogenous PGE2 to FATP2 KO PMN-MDSCs down-regulated the RIPK3 expression and successfully restored the RIPK3-PGE2 circuit. These results indicated that a synergy between FATP2 and RIPK3 pathways was mediated through PGE2. The PGE2-mediated synergy between FATP2 and RIPK3 pathways in PMN-MDSCs severely impaired the proliferation of $CD8^+$ T cells and inhibited the IFN-γ and Granzyme B expressions in $CD8^+$ T cells, while activating RIPK3 could effectively inhibited this effect (Fig. 5C, 5D and 5E). Similarly, the PGE2-mediated synergistic effect significantly promoted the synthesis of Arg-1 and PGE2 in PMN-MDSCs, and activating RIPK3 effectively inhibited this effect (Fig. 5F and 5G).

Effect of combination therapy with lipofermata and 666 − 15 on tumor-bearing mice.

To confirm whether combination therapy with inhibition of FATP2 and activation of RIPK3 can effectively inhibit tumor growth in vivo, lipofermata and 666 − 15 was used to inhibit the FATP2 and activate the RIPK3 expressions, respectively. As shown in Fig. 6A and 6B, combination therapy with lipofermata and 666 − 15 markedly inhibited the tumor growth and prolonged the survival time in the mouse model of bladder cancer.

Discussion

The immunosuppressive cells existing in the tumor microenvironment lead to tumor immune tolerance and treatment failure [12,13]. Inhibiting the activity of these immunosuppressive cells is the key to improving the efficacy of immunotherapy [14,15]. The infiltration of PMN-MDSCs in tumor microenvironment is closely related to poor prognosis [16]. PMN-MDSCs exert immunosuppressive functions via multiple signal pathways, such as secreting inhibitory cytokines (IL-1, IL-6, IL-10, and TGF-β) [17], inducing the expression of Arg-1 and iNOS [18], expressing a series of reactive oxygen species ROS [19], and inducing the production of $CD25^+$ $FOXP3^+$ Treg cells [20]. Inhibiting the immunosuppressive activity of PMN-MDSCs may be an effective way to improve anti-tumor immunity [21]. Therefore, it is of great significance to further explore the related mechanisms by which PMN-MDSCs exerts immunosuppressive functions.

In recent years, several studies have shown that both FATP2 and RIPK3 play a key role in promoting the suppressive activity of PMN-MDSCs [7,8]. Both FATP2 and RIPK3 enhance the suppressive activity of PMN-MDSCs by promoting the synthesis of PGE2, which is an important immunosuppressive molecule in maintaining the immunosuppressive activity of PMN-MDSCs [22]. In the study, we also found that a large number of PMN-MDSCs existed in the tumor microenvironment, and PMN-MDSCs infiltration significantly

correlated with FATP2 and RIPK3 expression. This phenomenon also exists in the tumor microenvironment of human bladder cancer. Moreover, FATP2 and RIPK3 expression was correlated with clinical stage, which indicated that overexpressed FATP2 and underexpressed RIPK3 were associated with poor prognosis.

Despite the fact that PMN-MDSCs and neutrophils share same origin and the same differentiation pathways, PMN-MDSCs have distinct genomic and biochemical features and are immunosuppressive [23]. When compared with PMNs, FATP2 expression was significantly up-regulated in PMN-MDSCs, while RIPK3 expression was significantly down-regulated. More interestingly, PMN-MDSCs isolated from tumor tissue showed higher FATP2 expression and lower RIPK3 expression than PMN-MDSCs isolated from spleen. This phenomenon has also been reported by a previous study [8]. At present, the specific mechanism by which this phenomenon occurs in the tumor microenvironment remain largely unknown.

FATP2 is a key molecule that regulates lipid metabolism in PMN-MDSCs [7]. Abnormal lipid metabolism could contribute to pathological activation of PMN-MDSCs [24]. An accumulation of lipids in cancer has been shown in macrophages [25], dendritic cells (DC) [26], and total population of MDSCs where it was associated with immunosuppressive activity [27]. A previous study have reported that FATP2 enhanced the suppressive activity of PMN-MDSCs by promoting arachidonic acid utilization and PGE2 synthesis [7]. In this study, FATP2 KO significantly decreased arachidonic acid and arachidonic acid metabolite PGE2 in PMN-MDSCs and seriously impaired the immunosuppressive effect of PMN-MDSCs on $CD8^+$ T cells. At present, although STAT5 has been reported to be one of the key molecules regulating FATP2 expression [7], the mechanism that regulates FATP2 still not fully understood.

RIPK3, as a key regulator of programmed cell necrosis, plays an important role in both inflammation and tumors [28]. RIPK3 was negatively correlated with tumor stage and is an important prognostic factor for colon cancer [29]. Recently, a previous study revealed the regulatory mechanism of a RIPK3-PGE2 circuit in PMN-MDSCs [8]. Lacking RIPK3 PMN-MDSCs had a stronger immunosuppressive activity. RIPK3 reduction activated the NF-κB-COX2-PGE2 signaling pathway and promoted PGE2 synthesis. The PGE2 further inhibited the expression of RIPK3 and promoted the NF-kB/COX-2 and Arg-1 expression through the cAMP/PKA-CREB signaling pathway, thus forming the RIPK3-PGE2 circuit. In the tumor microenvironment, PMN-MDSCs significantly promoted the PGE2 synthesis through the RIPK3-PGE2 circuit, thereby enhancing the immunosuppressive activity of PMN-MDSCs. As shown by the results of this study, breaking the RIPK3-PGE2 circuit by up-regulating RIPK3 significantly reduced the synthesis of PGE2 and further inhibited the immunosuppressive activity of PMN-MDSCs.

In PMN-MDSCs, both FATP2 and RIPK3 pathways could synthesize the PGE2 [8,30]. The PGE2 synthesized by the FATP2 pathway could further promote the synthesis of PGE2 through the RIPK3-PGE2 circuit, so the RIPK3-PGE2 circuit might be an amplifier of the FATP2 pathway in terms of promoting PGE2 synthesis. In vitro, FATP2 KO significantly up-regulated the RIPK3 expression and reduced PGE2 synthesis in PMN-MDSCs. However, after exogenous PGE2 stimulation, FATP2 KO PMN-MDSCs could also synthesize PGE2. In vivo, PGE2 is derived not only from MDSCs but also from tumor cells or other

cells [31]. Blocking FATP2 partially reduced the PGE2 synthesis of PMN-MDSCs, but it cannot completely inhibit the PGE2 synthesis in vivo. There was a synergy between FATP2 and RIPK3 pathways in promoting the PGE2 synthesis of PMN-MDSCs. Therefore, blocking the FATP2 and RIPK3 pathways at the same time can successfully minimize the synthesis of PGE2 in PMN-MDSCs. Our in vitro experiments also confirmed that blocking the FATP2 combined with up-regulating the RIPK3 minimized the PGE2 synthesis of PMN-MDSCs even adding exogenous PGE2.

In this study, there are some shortcomings. This study initially proved that there were a large number of PMN-MDSCs in tumor tissues, and the expression of FATP2 was down-regulated, and RIPK3 was down-regulated. However, this study has not yet elucidated the molecular mechanism that causes this phenomenon in the tumor microenvironment. Elucidating the molecular mechanism is likely to help discover more effective therapeutic targets to overcome PMN-MDSCs-mediated immune escape. In addition, the clinical sample size included in this study is small, and a larger sample is needed to verify the conclusions of the study.

In summary, our results demonstrated that the synergy between FATP2 and RIPK3 pathways in PMN-MDSCs significantly promoted the synthesis of PGE2, which severely impaired the $CD8^+$ T cell function and IFN-γ secretion. Combination therapy with targeting FATP2 and RIPK3 might be considered for rational treatment for inhibiting the immunosuppressive activity of PMN-MDSCs and enhancing the antitumor immunity. These findings provided the molecular basis and potential ideas for the immunotherapy of bladder cancer.

Declarations

Author contributions Xiaojun Shi and Wanlong Tan conceived of this study, collected data, and prepared the manuscript. Jie Sun, Shiyu Pang and Jiawei Zhou collected data, performed data analysis, and prepared the manuscript. Guang Yan and Wanlong Tan collected data and revised the manuscript.

Funding This study was supported by National Natural Science Foundation of China (No.81902595) and China Postdoctoral Science Foundation (No.2018M640801).

Conflict of interest The authors declare that have no conflict of interest.

Ethical approval The study was approved by the Ethics Committee of Nanfang hospital. All patients signed the approved consent forms. All experimental procedures were performed in accordance with the relevant laws and institutional guidelines of Southern Medical University.

References

1. Siegel RL, Miller KD, Jemal A (2018) Cancer Statistics, 2018. CA Cancer J Clin 68 (1): 7-30.
2. Reeves E, James E (2-17) Antigen processing and immune regulation in the response to tumours. Immunology 150(1):16-24.

3. Giese MA, Hind LE, Huttenlocher A (2019) Neutrophil plasticity in the tumor microenvironment. Blood 133(20):2159-2167.
4. Yamauchi Y, Safi S, Blattner C, Rathinasamy A, Umansky L, Juenger S, et al (2018) Circulating and Tumor Myeloid-derived Suppressor Cells in Resectable Non-Small Cell Lung Cancer. Am J Respir Crit Care Med 198(6):777-787.
5. Zhang H, Li ZL, Ye SB, Ouyang LY, Chen YS, He J, et al (2015) Myeloid-derived suppressor cells inhibit T cell proliferation in human extranodal NK/T cell lymphoma: a novel prognostic indicator. Cancer Immunol Immunother 64(12):1587-99.
6. Nan J, Xing YF, Hu B, Tang JX, Dong HM, He YM, et al (2018) Endoplasmic reticulum stress induced LOX-1+CD15+ polymorphonuclear myeloid-derived suppressor cells in hepatocellular carcinoma. Immunology 154(1):144-155.
7. Veglia F, Tyurin VA, Blasi M, De Leo A, Kossenkov AV, Donthireddy L, et al (2019) Fatty acid transport protein 2 reprograms neutrophils in cancer. Nature 569(7754):73-78.
8. Yan G, Zhao H, Zhang Q, Zhou Y, Wu L, Lei J, et al (2018) A RIPK3-PGE2 Circuit Mediates Myeloid-Derived Suppressor Cell-Potentiated Colorectal Carcinogenesis. Cancer Res 78(19): 5586-5599.
9. Black PN, Ahowesso C, Montefusco D, Saini N, DiRusso CC (2016) Fatty Acid Transport Proteins: Targeting FATP2 as a Gatekeeper Involved in the Transport of Exogenous Fatty Acids. Medchemcomm 7(4):612-622.
10. Moriwaki K, Chan FK (2017) The Inflammatory Signal Adaptor RIPK3: Functions Beyond Necroptosis. Int Rev Cell Mol Biol 328:253-275.
11. Evans AS, Coyne CB (2019) RIPK3: Beyond Necroptosis. Immunity 50(1):1-3.
12. Cunha LD, Yang M, Carter R, Guy C, Harris L, Crawford JC, et al (2018) LC3-Associated Phagocytosis in Myeloid Cells Promotes Tumor Immune Tolerance. Cell 175(2):429-441.e16.
13. Costa A, Kieffer Y, Scholer-Dahirel A, Pelon F, Bourachot B, Cardon M, et al (2018) Fibroblast Heterogeneity and Immunosuppressive Environment in Human Breast Cancer. Cancer Cell 33(3):463-479.e10.
14. Sawa-Wejksza K, Kandefer-Szerszeń M (2018) Tumor-Associated Macrophages as Target for Antitumor Therapy. Arch Immunol Ther Exp (Warsz) 66(2):97-111.
15. Fleming V, Hu X, Weber R, Nagibin V, Groth C, Altevogt P, et al (2018) Targeting Myeloid-Derived Suppressor Cells to Bypass Tumor-Induced Immunosuppression. Front Immunol 9:398.
16. Deng G (2018) Tumor-infiltrating regulatory T cells: origins and features. Am J Clin Exp Immunol 7(5):81-87.
17. Chen J, Ye Y, Liu P, Yu W, Wei F, Li H, et al (2017) Suppression of T cells by myeloid-derived suppressor cells in cancer. Hum Immunol 78(2):113-119.
18. Qu J, Liu L, Xu Q, Ren J, Xu Z, Dou H, et al (2019) CARD9 prevents lung cancer development by suppressing the expansion of myeloid-derived suppressor cells and IDO production. Int J Cancer 145(8):2225-2237.

19. Ohl K, Tenbrock K (2018) Reactive Oxygen Species as Regulators of MDSC-Mediated Immune Suppression. Front Immunol 9:2499.
20. Holmgaard RB, Zamarin D, Li Y, Gasmi B, Munn DH, Allison JP, et al (2015) Tumor-Expressed IDO Recruits and Activates MDSCs in a Treg-Dependent Manner. Cell Rep 13(2):412-24.
21. Uehara T, Eikawa S, Nishida M, Kunisada Y, Yoshida A, Fujiwara T, et al (2019) Metformin induces CD11b+-cell-mediated growth inhibition of an osteosarcoma: implications for metabolic reprogramming of myeloid cells and anti-tumor effects. Int Immunol 31(4):187-198.
22. Rodríguez-Ubreva J, Català-Moll F, Obermajer N, Álvarez-Errico D, Ramirez RN, Company C, et al (2017) Prostaglandin E2 Leads to the Acquisition of DNMT3A-Dependent Tolerogenic Functions in Human Myeloid-Derived Suppressor Cells. Cell Rep 21(1):154-167.
23. Giese MA, Hind LE, Huttenlocher A (2019) Neutrophil plasticity in the tumor microenvironment. Blood 133(20):2159-2167.
24. He YM, Li X, Perego M, Nefedova Y, Kossenkov AV, Jensen EA, et al (2018) Transitory presence of myeloid-derived suppressor cells in neonates is critical for control of inflammation. Nat Med 24(2):224-231.
25. Voloshyna I, Teboul I, Kasselman LJ, Salama M, Carsons SE, DeLeon J, et al (2019) Macrophage lipid accumulation in the presence of immunosuppressive drugs mycophenolate mofetil and cyclosporin A. Inflamm Res 68(9):787-799.
26. Arai R, Soda S, Okutomi T, Morita H, Ohmi F, Funakoshi T, et al (2018) Lipid Accumulation in Peripheral Blood Dendritic Cells and Anticancer Immunity in Patients with Lung Cancer. J Immunol Res 2018:5708239.
27. Niavarani SR, Lawson C, Bakos O, Boudaud M, Batenchuk C, Rouleau S, et al. Lipid accumulation impairs natural killer cell cytotoxicity and tumor control in the postoperative period. BMC Cancer. 2019;19(1):823.
28. Newton K, Manning G (2016) Necroptosis and Inflammation. Annu Rev Biochem 85:743-763.
29. Conev NV, Dimitrova EG, Bogdanova MK, Kashlov YK, Chaushev BG, Radanova MA, et al (2019) RIPK3 expression as a potential predictive and prognostic marker in metastatic colon cancer. Clin Invest Med 42(1):E31-E38.
30. Riegger J, Brenner RE (2019) Evidence of necroptosis in osteoarthritic disease: investigation of blunt mechanical impact as possible trigger in regulated necrosis. Cell Death Dis 10(10):683.
31. Elwakeel E, Brüne B, Weigert A (2019) PGE2 in fibrosis and cancer: Insights into fibroblast activation. Prostaglandins Other Lipid Mediat 143:106339.

Figures

Figure 1

PMN-MDSCs, overexpressed FATP2 and underexpressed RIPK3 in the tumor microenvironment.

(A) Immunofluorescence assays were performed to detect the PMN-MDSCs with anti-CD11b (red) and anti-LOX-1 (green) antibodies. Tumor cell nuclei were stained with DAPI (blue). The double positive cells ($CD11b^{+}LOX\text{-}1^{+}$) (yellow) were considered to be PMN-MDSCs (bar = 200 um). (B and C) Immunohistochemistry assays of FATP2 and RIPK3 proteins with anti-FATP2 or anti-RIPK3 antibody (bar = 200 um). (D and E) Correlation analysis between the number of PMN-MDSCs and FATP2 or RIPK3 expression in tumor tissues. (F) Expressions of LOX-1, FATP2 and RIPK3 in human bladder cancer tissues and adjacent tissues. (G) Expressions of FATP2 and RIPK3 were significantly correlated with clinical stage. (* $P < 0.05$)

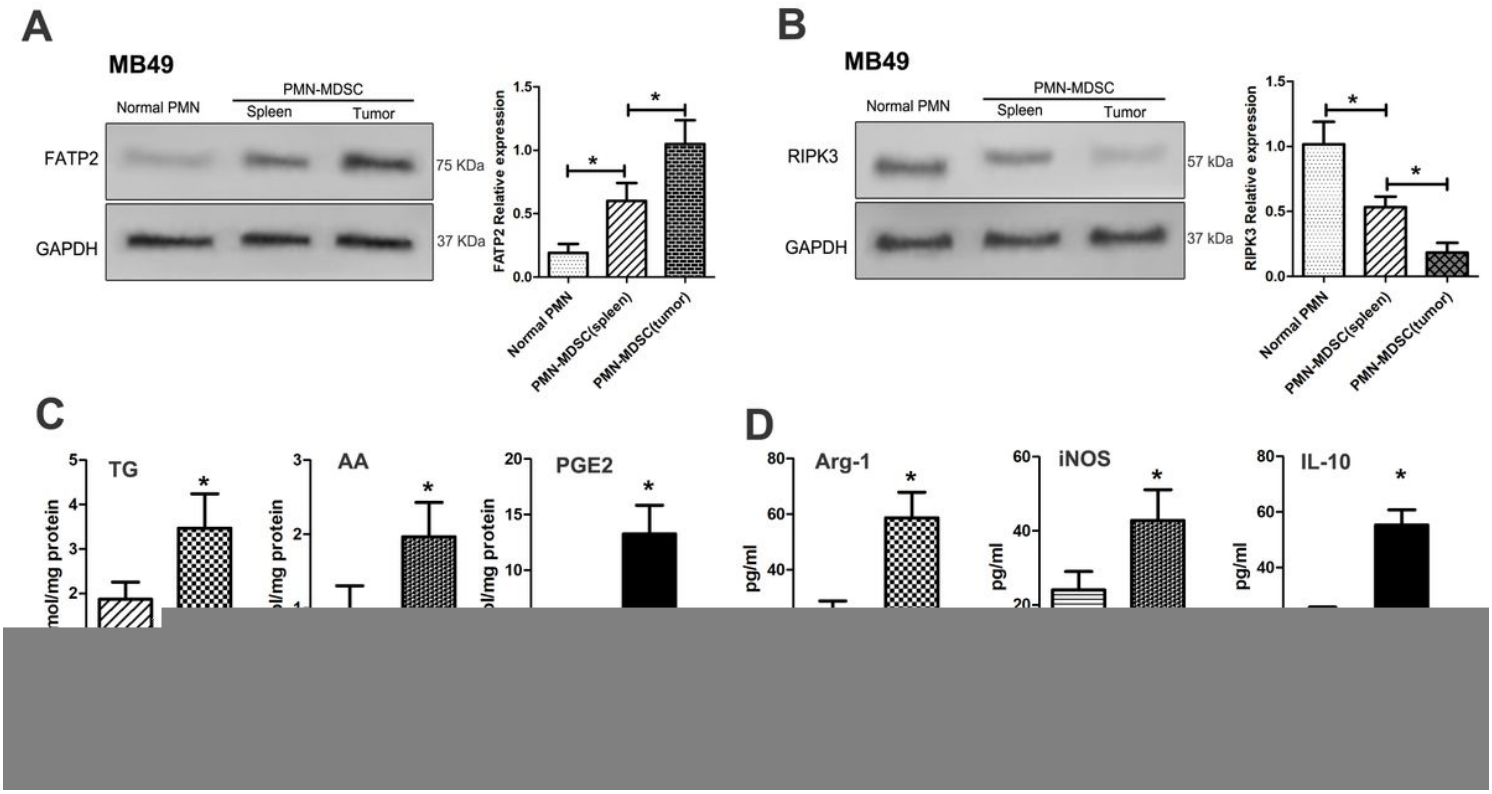

Figure 2

Overexpressed FATP2 and underexpressed RIPK3 in PMN-MDSCs.

(A) Western blotting detected the FATP2 expression in PMN-MDSCs isolated from spleen and tumor tissue. (B) Western blotting detected the RIPK3 expression in PMN-MDSCs isolated from spleen and tumor tissue. (C) LC/MS detected the triglycerides (TG), arachidonic acid (AA), prostaglandin E2 (PGE2) in PMN-MDSCs from tumor-bearing mice or PMNs from normal mice. (D) The immunosuppressive molecules (Arg-1, INOS, IL-10) in PMN-MDSCs or PMNs were detected by ELISA. (*P<0.05)

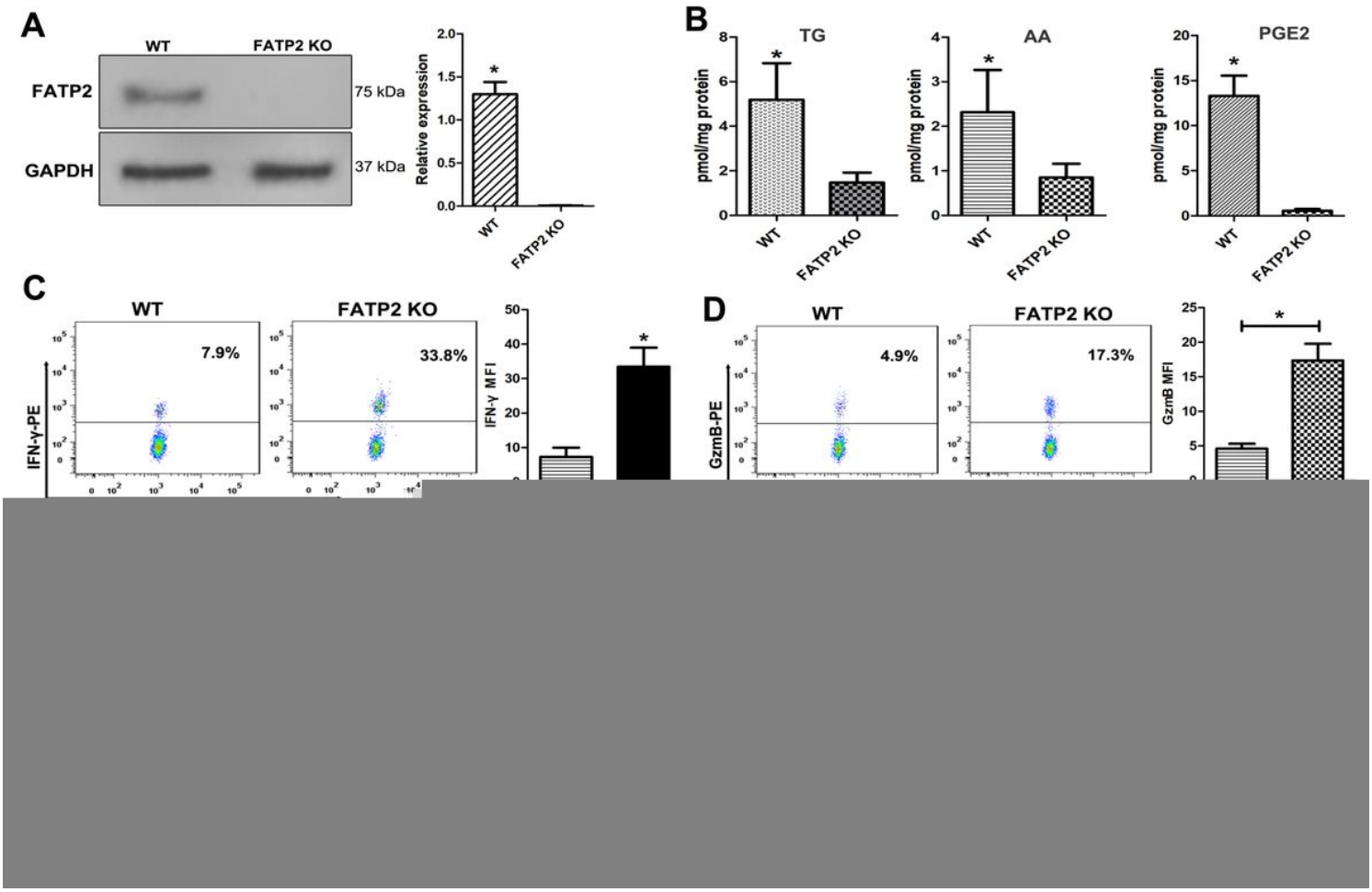

Figure 3

Effects of FATP2 KO on the functions of PMN-MDSCs.

(A) Western blotting detected the FATP2 expression in WT and FATP2 KO PMN-MDSCs. (B) LC-MS detected the TG, AA and PGE2 in WT and FATP2 KO PMN-MDSCs. (C and D) Flow cytometry detected the IFN-γ and Granzyme B expressions in $CD8^+$ T cells co-cultured with WT and FATP2 KO PMN-MDSCs. (E) CFSE ananlysis was performed to evaluated the proliferation of $CD8^+$ T cells co-cultured with WT and FATP2 KO PMN-MDSCs. (F) FATP2 KO effectively inhibited tumor growth in mice. (* $P < 0.05$)

Figure 4

Effects of RIPK3-activated on the functions of PMN-MDSCs.

(A) Western blotting detected the RIPK3 expression in RIPK3-activated PMN-MDSCs and control. (B) LC-MS detected the TG, AA and PGE2 in RIPK3-activated PMN-MDSCs and control. (C and D) Flow cytometry detected the IFN-γ and Granzyme B expressions in $CD8^+$ T cells co-cultured with RIPK3-activated PMN-MDSCs and control. (E) CFSE ananlysis was performed to evaluated the proliferation of $CD8^+$ T cells co-

cultured with RIPK3-activated PMN-MDSCs and control. (F) 666-15 (RIPK3-activated) effectively inhibited tumor growth in mice. (* $P < 0.05$)

Figure 5

Synergy between FATP2 and RIPK3 Pathways was mediated through PGE2.

(A and B) Western blotting detected the expressions of RIPK3-PGE2 circuit-related signaling proteins in WT, FATP2 KO PMN-MDSCs and PGE2-activated FATP2 KO PMN-MDSCs. (C) CFSE ananlysis was performed to evaluated the proliferation of $CD8^+$ T cells co-cultured with WT, FATP2 KO PMN-MDSCs and PGE2-activated FATP2 KO PMN-MDSCs. (D and E) Flow cytometry detected the IFN-γ and Granzyme B expressions in $CD8^+$ T cells co-cultured with WT, FATP2 KO PMN-MDSCs and PGE2-activated FATP2 KO PMN-MDSCs. (F and G) PGE2-mediated synergy between FATP2 and RIPK3 pathways in PMN-MDSCs promoted the synthesis of Arg-1 and PGE2. (* $P < 0.05$)

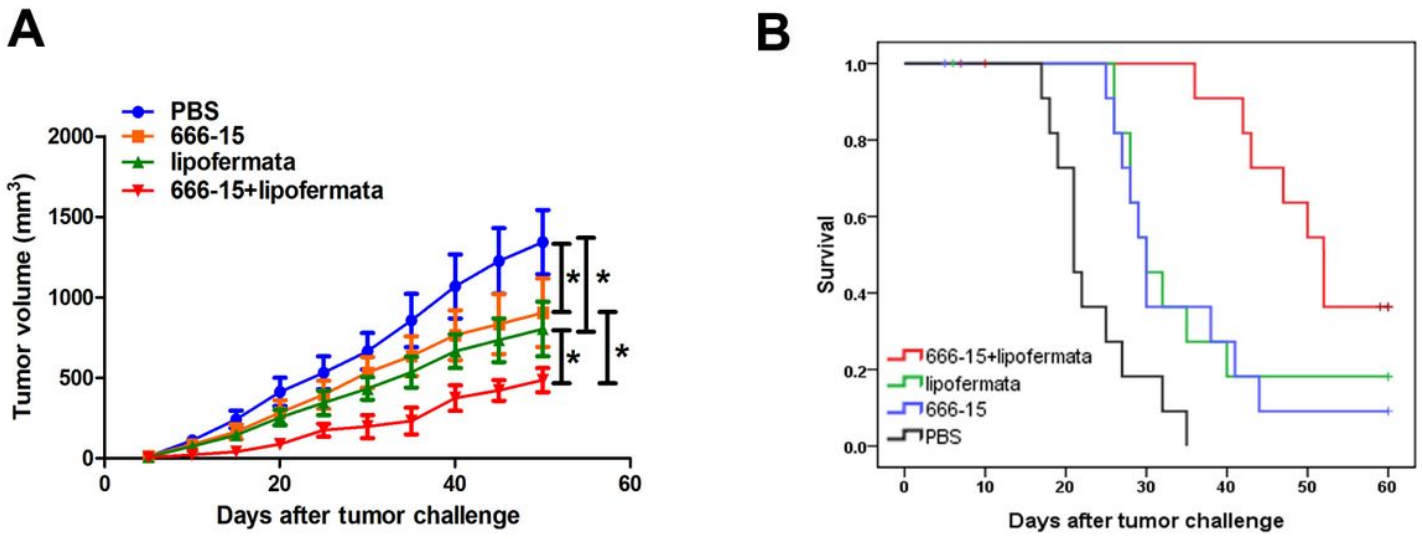

Figure 6

Effect of combination therapy with lipofermata and 666-15 on tumor-bearing mice.

Lipofermata and 666-15 was used to inhibit the FATP2 and activate the RIPK3 expressions, respectively. The tumor volume (A) and survival time (B) reflect the effects of combination therapy with lipofermata and 666-15 on tumor growth in the mouse model of bladder cancer. (*$P < 0.05$)